

An Effective Inverse Approach for Identifying an Impact Force Acting on CFRP Laminated Plates

N. Hu, H. Fukunaga
Tohoku University, Sendai, Japan

1. Introduction

It is well known that the composite laminates are suspicious to the various impact events. Therefore, it is crucial to monitor the external impact forces. In some previous studies for the impact force identification problem, the method using a transfer function has been proposed. For the cases with given force locations in advance, for example, Inoue *et al.* [1, 2] have experimentally obtained the transfer function between impact forces and strain responses, and determined the impact forces through the deconvolution method. Using the same relationship obtained numerically, Doyle [3] proposed the similar technique for identifying an impact force history in a time domain from the strain response. The technique was further extended to the identification in a frequency domain using FFT. [4]. In addition, the validity of this method was verified through experiments using strain gauges. Wu *et al.* [5] have constructed Green's functions with the eigenmode expansion method and identified impact force histories by minimizing the residual error between measured strain responses and numerically evaluated ones. However, the accurate and stable methods are still needed. In this paper, we propose a simple, fast and efficient method in order to identify the location and history of a low velocity impact force. First, the impact force history is approximated by Chebyshev polynomial. The identification of force histories is achieved by solving an inverse problem through the quadratic programming optimum method. Furthermore, in the present approach, the impact force location is obtained by directly comparing the experimental strains with the numerical strains. The merits of the present method are its low computational cost and high accuracy. The present method is applied to two kinds of cantilevered CFRP plates with a thin network in which PZT piezoelectric sensors are embedded. The experimental results are reported and the validity of the present method is verified.

2. Theory

To obtain the stable and reliable impact force history, the basic idea in this study is to employ a series of smooth functions to approximate the force history. We have found that Chebyshev polynomial is very effective due to its fast convergence in the practical impact force identification. In this study, we adopt this kind polynomial. First, Chebyshev polynomial of degree k is denoted by $C_k(\xi)$, and is given by the explicit form as follows:

$$C_k(\xi) = \cos(k \arccos(\xi)) \quad (1)$$

In usual cases, Chebyshev polynomial is defined within the band $[-1,1]$ for ξ . To map this band into the time domain of $[0, T]$, the following relationship is used:

$t=[2\xi-T]/T$. Therefore, $C_k(\xi)$ changes into $C_k^*(t)$, and we can approximate the impact force as follows

$$P(t) = \sum_{k=1}^K \beta_k C_k^*(t) \quad (2)$$

where K is the number of base functions employed in Chebyshev polynomial.

By employing the mode superposition method, after obtaining the modal data of the original system, the modal displacement can be estimated as follows

$$\begin{aligned} \mathcal{G}_i(t) &= \frac{\boldsymbol{\Phi}_i^T \mathbf{P}}{\omega_i(\sqrt{1-\zeta^2})} \int_0^t P(\tau) e^{-\zeta\omega_i(t-\tau)} \sin[\omega_i\sqrt{1-\zeta^2}(t-\tau)] d\tau \\ &= \boldsymbol{\Phi}_i^T \mathbf{p} \sum_{k=1}^K S_k^i(t) \beta_k \end{aligned} \quad (3)$$

where \mathbf{p} is the load vector containing the information of load location, $\boldsymbol{\Phi}_i$ is the i th vibration mode, ω_i is the i th circular frequency of system and ζ is the damping parameter. And

$$S_k^i(t) = \frac{\int_0^t C_k^*(\tau) e^{-\zeta\omega_i(t-\tau)} \sin[\omega_i\sqrt{1-\zeta^2}(t-\tau)] d\tau}{\omega_i(\sqrt{1-\zeta^2})} \quad (4)$$

Finally, the displacements in the time domain can be obtained using the mode superposition method as follows

$$\mathbf{u}(t) = \sum_{i=1}^N \boldsymbol{\Phi}_i \mathcal{G}_i(t) = \sum_{i=1}^N \boldsymbol{\Phi}_i \boldsymbol{\Phi}_i^T \mathbf{p} \left(\sum_{k=1}^K S_k^i(t) \beta_k \right) = \boldsymbol{\Phi}(t) \boldsymbol{\eta} \quad (5)$$

where N is the number of modal data, and

$$\boldsymbol{\Phi}(t) = \left[\sum_{i=1}^N \boldsymbol{\Phi}_i \boldsymbol{\Phi}_i^T \mathbf{p} S_1^i \quad \sum_{i=1}^N \boldsymbol{\Phi}_i \boldsymbol{\Phi}_i^T \mathbf{p} S_2^i \quad \dots \quad \sum_{i=1}^N \boldsymbol{\Phi}_i \boldsymbol{\Phi}_i^T \mathbf{p} S_K^i \right] \quad (6)$$

and $\boldsymbol{\eta}$ is the vector containing unknown coefficients in Chebyshev polynomial $\boldsymbol{\eta} = [\beta_1 \ \beta_2 \ \dots \ \beta_K]^T$.

Consider L discrete time points within the time domain $[0, T]$, for the i th sensor, the strain data at these time points can be listed as

$$\begin{aligned} \boldsymbol{\varepsilon}_i^C &= [\varepsilon_i^C(t_1) \ \varepsilon_i^C(t_2) \ \dots \ \varepsilon_i^C(t_L)] \\ &= [\mathbf{T}_i \boldsymbol{\Phi}(t_1) \boldsymbol{\eta} \quad \mathbf{T}_i \boldsymbol{\Phi}(t_2) \boldsymbol{\eta} \quad \dots \quad \mathbf{T}_i \boldsymbol{\Phi}(t_L) \boldsymbol{\eta}] = \mathbf{A}_i \boldsymbol{\eta} \end{aligned} \quad (7)$$

By comparing this strain data $\boldsymbol{\varepsilon}_i^C$ with the experimental ones $\boldsymbol{\varepsilon}_i^*$ at L discrete time points within the time domain $[0, T]$ of S sensors, we can set up the following optimum model

$$\min \sum_{i=1}^S \left\| \mathbf{A}_i \boldsymbol{\eta} - \boldsymbol{\varepsilon}_i^* \right\|^2 \quad (8a)$$

s.t.

$$f(0) = \sum_{k=1}^K [C_k^*(0) \beta_k] = 0.0 \quad (8b)$$

$$f(t_n) = \sum_{k=1}^K [C_k^*(t_n)\beta_k] \geq 0.0 \quad (n=1 \cdots L) \quad (8c)$$

where Eq. (8b) is the constraint condition to enforce the impact force to be zero at $t=0$, and Eq. (8c) is the one to enforce the impact force to be compressive load within the time domain.

By solving the above optimization model using the quadratic programming method, we can get $\boldsymbol{\eta}$, and then construct the impact force history using Eq. (2). Compared with the traditional method using the impact force at discrete time points as unknowns, the property of the above inverse problem, i.e. the property of the matrix $\mathbf{A}_i^T \mathbf{A}_i$, is improved due to introduction of smooth Chebyshev base functions. The number of unknowns is reduced significantly since only a few base functions are needed to get the converged results. The obtained impact force history is very stable as shown in experimental verifications.

After solving Eq. (8), we can get $\boldsymbol{\eta}$ at the assumed force location. Now, the error vector $\tilde{\boldsymbol{\varepsilon}}$ can be defined as

$$\tilde{\boldsymbol{\varepsilon}} = \sum_{i=1}^S \|\mathbf{A}_i \boldsymbol{\eta} - \boldsymbol{\varepsilon}_i^*\|^2 / \sum_{i=1}^S \|\boldsymbol{\varepsilon}_i^*\|^2 \quad (9)$$

This error indicates a deviation between the measured strain responses and the strain responses evaluated using the numerical model from the temporarily identified impact force history, denoted by $\boldsymbol{\eta}$. Thus, the true location of impact force can be determined from the possible impact locations by solving a minimum problem defined in the following equation

$$\min \tilde{\boldsymbol{\varepsilon}} \quad (10)$$

The direct parametric search in all of possible impact locations is employed for Eq. (1). Once the true location is determined when $\tilde{\boldsymbol{\varepsilon}}$ reaches at the minimum, the corresponding force history can be taken as the true force history.

3. System of Impact Force Identification

3.1 Experimental setup

The experimental system for verifying the present method is shown in Fig. 1. The identification system consists of a cantilevered CFRP plate specimen, a jig, a charge amplifier, a digital oscilloscope and a personal computer. In the experimental setup shown in Fig. 2, the CFRP plate is clamped by fastening a few bolts on the jig. Two kinds of CFRP plates are considered in the present research as shown in Table 1. The material properties are shown in Table 2. A strain sensor network called SMART Layer (Accellent Technology, Inc.), in which 4 PZT sensors are arranged, is utilized to measure strain responses. This layer is embedded with the laminate and near the bottom surface of the plate with the distance of 0.3 mm. The sensors are located at (85, 90), (213, 90), (86, 216) and (213, 218) mm in the plate plane. The schematic illustration of the shape of specimen and sensor positions is in Fig. 3.

On the other hand, the impact is applied using an impulse hammer (ONO

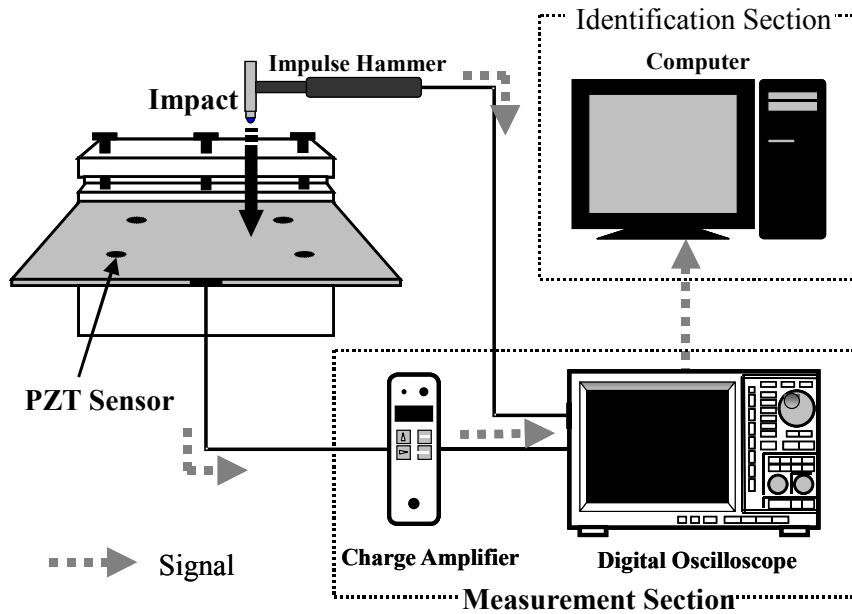


Fig. 1. System of impact force identification

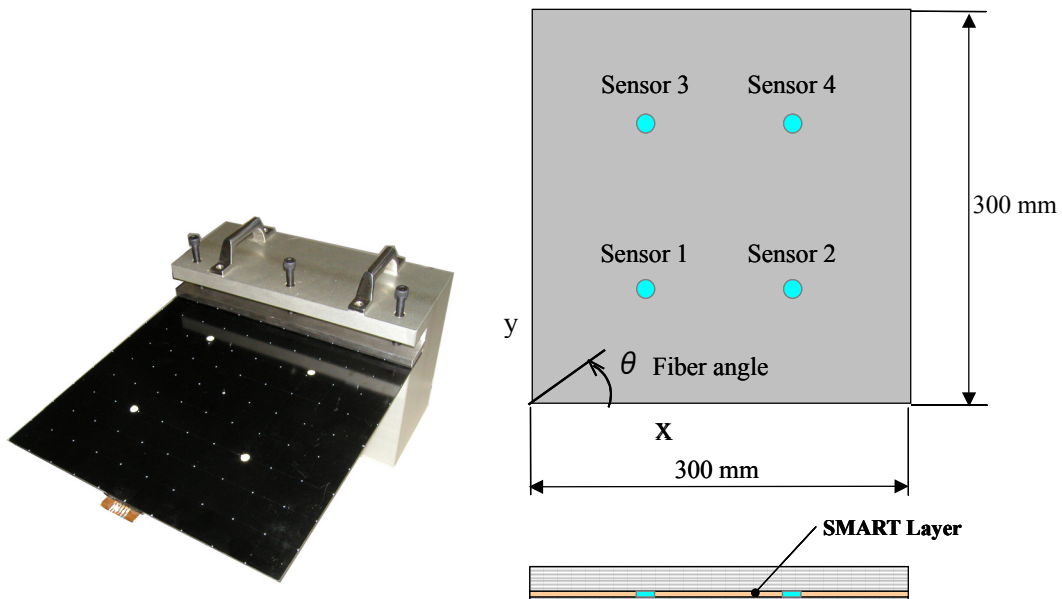


Fig. 2. Specimen and jig Fig. 3. Shape of specimen and sensor positions

SOKKI, GK-3100). Multiple sensor responses due to the applied impact are amplified through a charge amplifier (ONO SOKKI, CH-1100), and A/D conversion is conducted through a digital oscilloscope (YOKOGAWA, DL708E).

Finally, strain responses are inputted into a personal computer. The response of the impulse hammer measured coincidentally is also stored in the computer for comparison. In this study, the total measurement time is 0.1 sec and the sampling

Table 1. Properties of the specimens

CFRP1	CFRP2
Geometry (Rectangular)	
Length = 299.8 [mm] Width = 299.8 [mm]	Length = 300.2 [mm] Width = 299.8 [mm]
Stacking sequence	
$[45_2 / -45_4 / 45_2]_s$	$[0_2 / 45_2 / -45_2 / 90_2]_s$

Table 2. Properties of the lamina

Thickness	0.125 mm
E_L	142 GPa
E_T	10.8 GPa
G_{LT}	5.49 GPa
Poisson's Ratio	0.30
Density	1,600 kg/m ³

time Δt is 0.0001 sec. For the force history and location identification, the strain information within the first 0.0135 sec is employed.

3.2 Finite element model

The finite element model of 9×10 division consisting of 90 elements is shown in Fig. 4. All possible impact locations are also numbered in this figure, where the sensor positions and nodes at the plate edges are avoided as the impact positions. The 4-noded non-conforming bending element based on Kirchhoff plate theory is employed, which is of three degrees of freedom at each node, i.e., the deflection w , rotation around y -axis θ_x and rotation around x -axis θ_y . In the experimental setup in Fig. 2, the CFRP plate is clamped by fastening a few bolts on the jag. Thus, the boundary conditions in Fig. 4 are imposed on 11 nodes, where all degrees of freedom of those nodes (■ in Fig. 4) along the edge of the plate, are fixed. On the other hand, in order to determine the necessary number of natural vibration modes used in Eq. (5), an experiment has been performed to obtain the frequency content, from which very low spectrum energy has been observed in the frequencies higher than 2kHz. Consequently, the first 30 natural vibration modes corresponding to the frequencies lower than 2kHz are employed in the present numerical analysis. Additionally, the effects of the thickness, the mass and the stiffness of SMART Layer on the finite element model are ignored and the direction of impact force is defined to be positive when an impact induces compressive strains on the lower surface. Also, the damping is neglected in the numerical model.

4. Identification Results

4.1 Convergence of number of Chebyshev polynomials

First, we have checked the necessary number of base functions in Chebyshev polynomial for obtaining the converged impact force history. When using the data of the first 135 time steps and 90 4-noded Kirchhoff bending elements, the comparison between the experimental result and the identified results are illustrated in Fig. 5 for various Chebyshev polynomials. From this figure, it can be found that the identified results are converged when the first 30 or 40 Chebyshev base functions are used. However, for the case of the first 20 Chebyshev base functions, the maximum identified impact force is a little lower than that obtained from the first 30 or 40 Chebyshev base functions. To reduce the identification

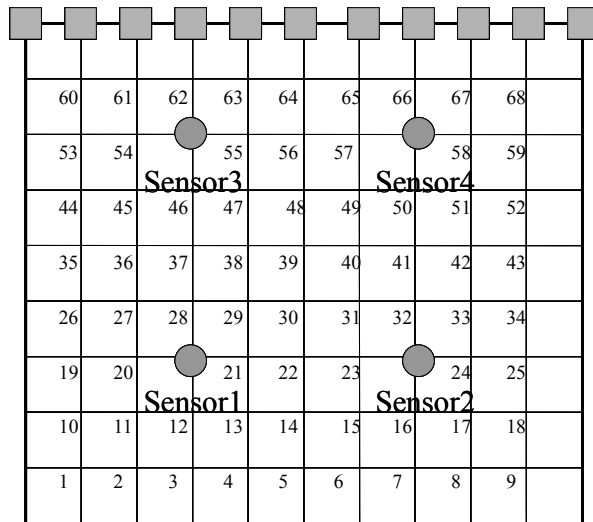


Fig. 4. FEM mesh and experimental impact points

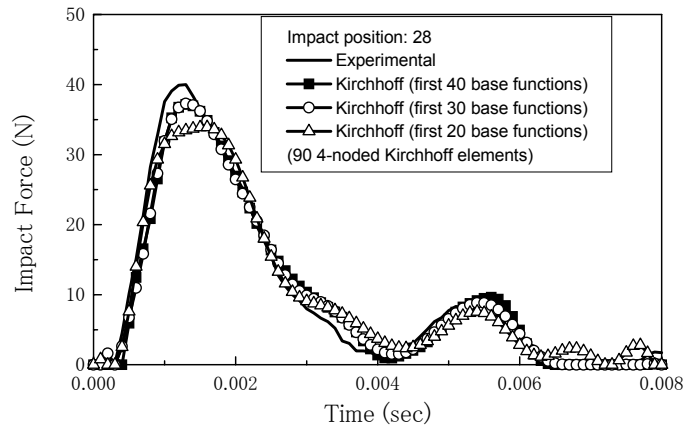


Fig. 5. Convergence of Chebyshev polynomials

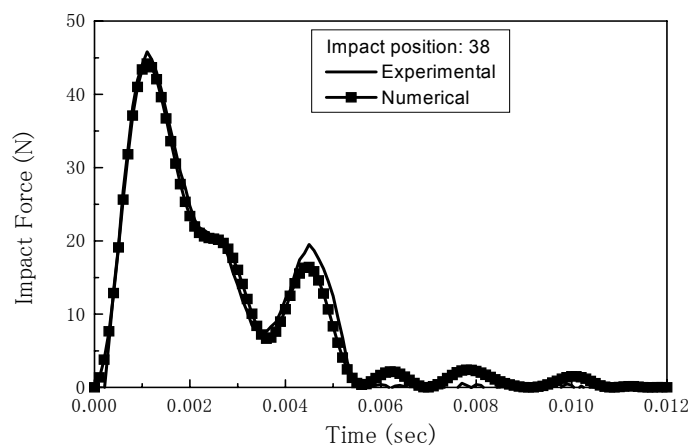


Fig. 6. Impact force histories for CFRP1 at 38

time, we employ the first 30 Chebyshev base functions in our following numerical

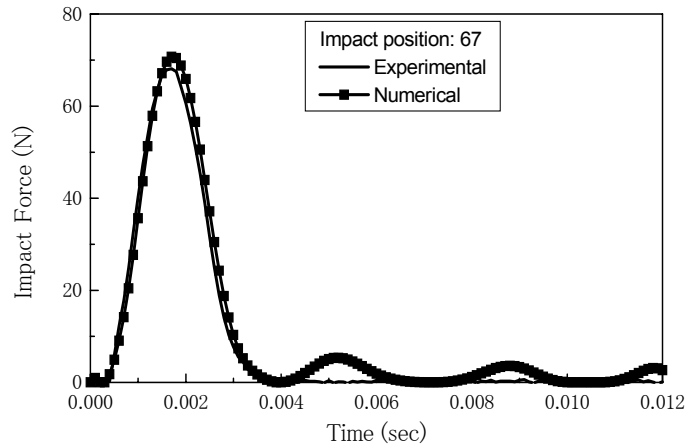


Fig. 7. Impact force histories for CFRP2 at 67

computations.

4.2 Impact force history

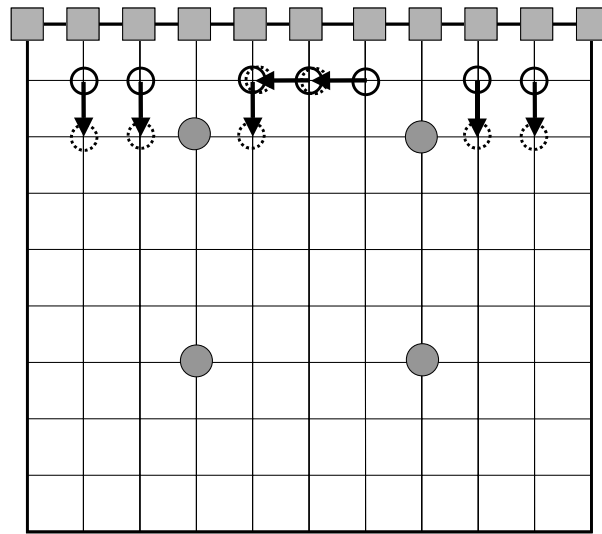
For CFRP1 defined in Table 1, the impact force histories for the impact positions of 38 shown in Fig. 4 are shown in Fig. 6. Inspection of this figure reveals that the impact force history can be identified very accurately although complex impact force history occurs. For CFRP2 defined in Table 1, the impact force histories for the impact positions of 67 shown in Fig. 4 are shown in Fig. 7. We can also see that the impact force histories can be identified accurately. Naturally, for some cases, especially, when the impact location is near the plate boundary, the accuracy of force history identification decreases. Sometimes, this inaccuracy is caused by the wrongly identified force location. Sometimes, even though the force location can be detected correctly, the accuracy in the force history identification is not as high as those shown in Figs 6 and 7.

4.3 Impact position

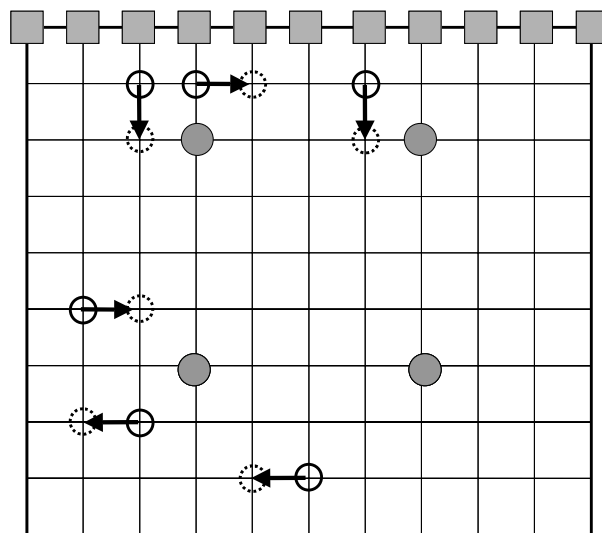
The results of identified impact locations are shown in Figs 8(a) and 8(b) for CFRP1 and CFRP2. For the most cases, the impact force locations can be identified successfully. Only those failed cases are shown in Figs 8(a) and 8(b). From Fig. 8(a), it can be found that the impact locations may be wrongly identified near the fixed edge. By observing Fig. 8(b), it can be found that the failed cases also appear near the free boundary besides those near the fixed edge. All of these failed cases may be mainly caused by the difference between the experimental model and numerical model, and the noises in the experimental data. From Figs 8(a) and 8(b), it can also be seen that the wrongly identified impact locations are very close to the true locations.

5. Conclusions

A simple and efficient technique for identifying the impact force is proposed in this research. Chebyshev polynomial is employed to model the impact force history. Based on the finite element method and the mode superposition method,



(a) CFRP1



(b) CFRP2

Fig. 8. Failed cases of identified impact force location (○ : true location; ⊖ : identified location)

the relation between the unknown parameters and the strain responses at the specified positions is formulated. An optimization model is constructed to obtain the impact force history by employing the quadratic programming method. This technique makes the solution of the impact force history very stable and accurate. After obtaining the impact force history, the impact location can be identified by minimizing the difference between the numerical strains and experimental ones. The experimental system for identifying the impact force, which includes two kinds of CFRP laminates with four embedded piezoelectric sensors, is set up to

validate the present methodology. From the obtained results, it can be found that the present method can produce the impact force history quickly and accurately. For the identification results of impact locations, only few cases cannot be identified successfully, which are near the fixed edge or free boundaries of plate. However, the wrongly identified force locations are very near the true locations.

References

- [1] H. Inoue, R. Watanabe, T. Shibuya, T. Koizumi, Measurement of impact force by the deconvolution method (part-a), *Journal of Japanese Society for Non-Destructive Inspection* 34 (1988) 337-342
- [2] H. Inoue, R. Watanabe, T. Koizumi, J. Fukuchi, Measurement of impact force applied to a plate by the deconvolution method (part-b), *Journal of Japanese Society for Non-Destructive Inspection* 37 (1988) 874-878
- [3] J.F. Doyle, An experimental method for determining the dynamic contact law. *Experimental Mechanics* 24 (1984) 10-16
- [4] J.F. Doyle, Experimentally determining the contact force during the transverse impact of an orthotropic plate, *Journal of Sound and Vibration* 118 (1987) 441-448
- [5] E. Wu, J.C. Yeh, C.S. Yen, Identification of impact forces at multiple locations on laminated plates, *AIAA Journal* 32 (1994) 2433-2439